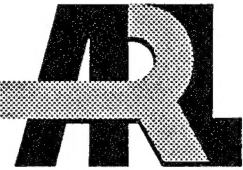ARMY RESEARCH LABORATORY

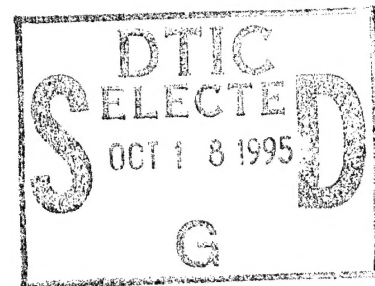# Current and Heat Transport in the Cannon-Caliber Electromagnetic Gun Armature

John D. Powell
Alexander E. Zielinski

ARL-MR-258                                                    August 1995

19951017 115

DTIC QUALITY INSPECTED 8

**NOTICES**

# REPORT DOCUMENTATION PAGE

Public reporting burden for this collection of information is estimated to average 1 hour per response, including the time for reviewing instructions, searching existing data sources, gathering and maintaining the data needed, and completing and reviewing the collection of information. Send comments regarding this burden estimate or any other aspect of this collection of information, including suggestions for reducing this burden, to Washington Headquarters Services, Directorate for Information Operations and Reports, 1215 Jefferson Davis Highway, Suite 1204, Arlington, VA 22202-4302, and to the Office of Management and Budget, Paperwork Reduction Project(0704-0188), Washington, DC 20503.

| 1. AGENCY USE ONLY (Leave blank) | 2. REPORT DATE | 3. REPORT TYPE AND DATES COVERED |
|---|---|---|
| | August 1995 | Final, October 1993 - December 1994 |

| 4. TITLE AND SUBTITLE | 5. FUNDING NUMBERS |
|---|---|
| Current and Heat Transport in the Cannon-Caliber Electromagnetic Gun Armature | PR: 1L162618AH80 |

**6. AUTHOR(S)**

John D. Powell and Alexander E. Zielinski

| 7. PERFORMING ORGANIZATION NAME(S) AND ADDRESS(ES) | 8. PERFORMING ORGANIZATION REPORT NUMBER |
|---|---|
| U.S. Army Research Laboratory<br>ATTN: AMSRL-WT-WD<br>Aberdeen Proving Ground, MD 21005-5066 | ARL-MR-258 |

| 9. SPONSORING/MONITORING AGENCY NAMES(S) AND ADDRESS(ES) | 10.SPONSORING/MONITORING AGENCY REPORT NUMBER |
|---|---|
| | |

**11. SUPPLEMENTARY NOTES**

| 12a. DISTRIBUTION/AVAILABILITY STATEMENT | 12b. DISTRIBUTION CODE |
|---|---|
| Approved for public release; distribution is unlimited. | |

**13. ABSTRACT (Maximum 200 words)**

A numerical model which we previously developed is extended and used to solve the equations which predict current and heat transport in a series-augmented, solid-armature railgun. The model is two-dimensional and fully time dependent. Specific calculations are carried out to analyze the armature recently designed and developed in the Cannon-Caliber Electromagnetic Launcher (CCEML) Program. The most extensive computations are for a situation in which the projectile is started at rest and accelerated to nearly 2 km/s in a time of 2 ms. Results of the calculations can be used to infer, for example, where melting in the armature is most likely to occur and where the electromagnetic stresses are largest. For comparison, calculations are also presented for a situation in which the projectile is held fixed. These calculations are intended to demonstrate the importance of velocity effects in the design of solid-armature railguns.

| 14. SUBJECT TERMS | | 15. NUMBER OF PAGES |
|---|---|---|
| railgun, electromagnetism, electromagnetic propulsion, electrodynamics, electromagnetic gun | | 25 |
| | | 16. PRICE CODE |

| 17. SECURITY CLASSIFICATION OF REPORT | 18. SECURITY CLASSIFICATION OF THIS PAGE | 19. SECURITY CLASSIFICATION OF ABSTRACT | 20. LIMITATION OF ABSTRACT |
|---|---|---|---|
| UNCLASSIFIED | UNCLASSIFIED | UNCLASSIFIED | UL |

INTENTIONALLY LEFT BLANK.

# TABLE OF CONTENTS

Accesion For

| NTIS   CRA&I | X |
| DTIC   TAB | ☐ |
| Unannounced | ☐ |
| Justification | |

By

Distribution /

Availability Codes

| Dist | Avail and / or Special |
| --- | --- |
| A-1 | |

INTENTIONALLY LEFT BLANK.

# LIST OF FIGURES

INTENTIONALLY LEFT BLANK.

# ACKNOWLEDGMENTS

INTENTIONALLY LEFT BLANK.

## 1. INTRODUCTION

In recent work (Powell, Walbert, and Zielinski 1993), we have developed a model and formalism for studying current and heat transport in solid-armature railguns. The model is two-dimensional and transient and can be used to determine the electromagnetic fields and forces, the current density, and the temperature in both the rails and the armature as a function of space and time. Such an analysis is important in order to guide the design of projectiles, in order to determine the limits under which these armatures can operate, and in order to study the dynamics of the armature and railgun.

In our previous work, we limited our study to the case of a small-bore, simple, single-turn railgun in which the current was carried from rail to rail via a U-shaped or slotted armature. In the present calculations, we will extend the model to treat the railgun and armature recently developed in the Cannon-Caliber Electromagnetic Gun (CCEMG) Program (Kitzmiller et al. 1994). The railgun has a rectangular bore cross section and is series augmented; the armature, which is discussed in more detail subsequently, is considerably more complicated than that which we have previously analyzed.

A schematic diagram of a series-augmented railgun, indicating the general principles on which it operates, is shown in Figure 1. Both sets of rails actually extend farther to the left and right of the armature than is shown in the figure, and are connected so as to produce equal currents in the directions indicated by the arrows. This configuration will produce an induction field in the bore to the left of the armature which is, in the two-dimensional case, exactly twice as large as that on the right. As a result, the total Lorentz force which accelerates the projectile is three times that which occurs in a simple railgun for any given value of the total current. The subject of concern here is to determine the distribution of current, the resulting body forces, and the generation and transport of heat everywhere in both the rails and armature.

Similar types of calculations for simple nonaugmented railguns and simple armatures have been undertaken by various investigators in the past. In early work, Young and Hughes (1982) investigated the current-diffusion problem analytically in the steady state for some rather simple types of armature geometry. Their work provided considerable insight into how the current could be expected to vary and the practical problems that would be encountered as the projectile velocity increased. Later, their work was extended to a transient analysis, and some limiting-case, exact solutions were obtained (Hughes and Young 1986). Similar transient, exact calculations have been undertaken by Nearing and Huerta (1989). Probably the most complete treatment of the problem is the work performed by Long (1986). His early analysis was somewhat similar to that of Hughes and Young, and succeeded in pre-
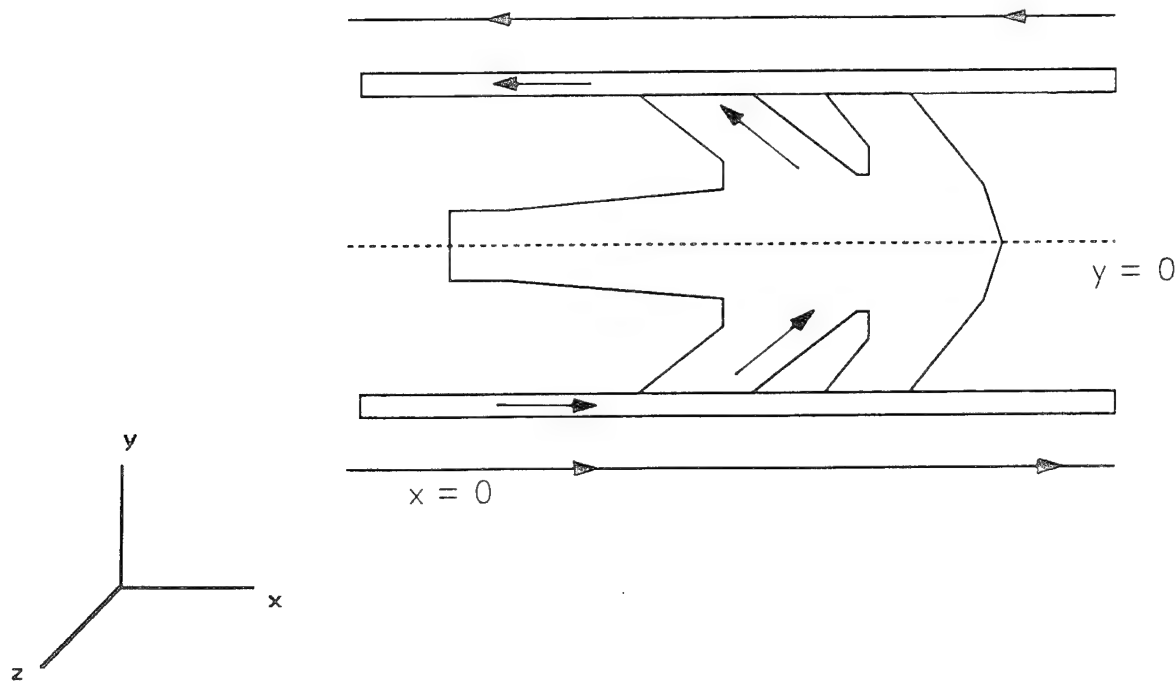
**Figure 1.** Schematic Diagram of a Series-Augmented, Solid-Armature Railgun.

dicting the current distribution analytically for simple armatures and rather low armature velocities in the steady state. In later graduate-thesis work, Long (1987) developed a finite-element program with which he successfully studied more complicated armatures at higher velocities. In addition, he included the effects of Joule heating, temperature-dependent electrical and thermodynamic properties, and heat transport, all of which had been neglected in the earlier analytic calculations. In more recent work, Putley (1989) adapted a previously developed code to solve the rail-armature interaction problem, verified some of Long's earlier calculations that were done analytically, and extended calculations to somewhat higher velocities. All of these calculations have been two-dimensional so that the rails were assumed to be infinitely high, with no variation in physical quantities along the direction of the rail height.

In addition to the two-dimensional work, there are important efforts underway to perform diffusion calculations in three dimensions. Recently, Yun and Price (1994) have performed a three-dimensional analysis on the CCEMG armature. The model which they employed, however, does not account for the motion of the launch package (i.e., $v = 0$). Early three-dimensional work which does account for conductor motion has been described in several references (Rodger, Leonard, Eastman, and Atkinson 1989; Rodger, Leonard, and Eastman 1991; Rodger and Leonard 1991), and additional efforts (Hsieh 1994) are currently

underway at the Institute for Advanced Technology to develop a three-dimensional finite-element code. Three-dimensional calculations, with appropriate models for physics at the rail-armature interface, should ultimately provide a realistic indication of the current and temperature distributions in railguns. These models can be used to avoid many assumptions of very limited applicability associated with the infinite rail-height calculations. However, the work is considerably more complicated than in two dimensions and is rather preliminary at this point.

The calculations to be undertaken here are most similar to those carried out by Long. We have developed a two-dimensional, finite-difference program which solves the governing equations for the fully transient case. Our motivation has been to provide information which could be used in the design of projectiles, as well as to provide information which could eventually be used as input in stress-analysis codes which have been developed to investigate in-bore dynamics. As indicated previously, the specific calculations described here will be for the armature recently developed as an integral part of the CCEMG Program. The organization of the report is as follows. In section 2, the model is described and the mathematical formalism developed. In section 3, we describe the results of some calculations for this specific armature geometry. Finally, section 4 contains our summary and conclusions.

## 2. MODEL AND FORMALISM

The basic equations that must be solved numerically consist of the appropriate Maxwell equations as well as the energy transport equation for the rails and projectile. It is convenient to solve these equations in a frame of reference in which the armature is fixed with its trailing edge located at $x = 0$ (see Figure 1), and the rails move in the negative $x$ direction. We will restrict ourselves to situations in which the armature is symmetric about a plane centered between the rails. This plane is defined by $y = 0$. The rails and projectile are infinitely extended in the $z$ direction. The governing equations to be developed are solved in the armature and the inner rails; the details concerning the outer rails are not considered except in the sense that they affect the boundary conditions on the magnetic induction as discussed previously.

Let $\vec{J}$, $\vec{B}$, and $\vec{E}$ be the current density, the magnetic induction field, and the electric field intensity. Let $\mu$, $\kappa$, $\sigma$, and $C$ be the magnetic permeability, the thermal conductivity, the electrical conductivity, and the specific heat. Finally, let $T$, $\rho$, and $v$ be the temperature, density, and material velocity at a given point in the rail-armature system. The governing Maxwell equations can then be written

$$\nabla \times \vec{B} = \mu \vec{J}, \tag{1}$$

$$\nabla \times \vec{E} = -\frac{\partial \vec{B}}{\partial t}, \tag{2}$$

and

$$\vec{J} = \sigma(\vec{E} + \vec{v} \times \vec{B}). \tag{3}$$

As is customary in calculations of this type, we have neglected the displacement current in equation (1). This approximation can be shown to be valid provided the armature velocity is small compared to the light speed c, and provided the time scale $\tau$ of the problem satisfies the condition $\tau \gg (\mu\sigma c^2)^{-1}$. Both these conditions are very easily satisfied for rail-launcher problems. Equation (3) represents Ohm's law in a moving conductor.

We now observe that for the infinite rail-height geometry discussed previously, we must have that $\vec{B} = B\hat{a}_z$ and that $J_z$ and $E_z$ both vanish. Furthermore, there can be no z dependence in any of the physical quantities. If we now make use of these observations, we find that equations (1)–(3) can be uncoupled to produce a single, second-order, partial differential equation which predicts the convection and diffusion of the magnetic induction field. The equation can be written

$$\mu\sigma\frac{\partial B}{\partial t} = \frac{\partial^2 B}{\partial x^2} + \frac{\partial^2 B}{\partial y^2} - \mu\sigma v\frac{\partial B}{\partial x} - \frac{1}{\sigma}\frac{\partial\sigma}{\partial T}\frac{\partial T}{\partial x}\frac{\partial B}{\partial x} - \frac{1}{\sigma}\frac{\partial\sigma}{\partial T}\frac{\partial T}{\partial y}\frac{\partial B}{\partial y}. \tag{4}$$

In obtaining equation (4), we have assumed that $\sigma$ depends on position and time only through the temperature $T$.

A similar assumption for $\kappa$ and $C$ allows us to write the heat-transport equation as

$$\rho C\frac{\partial T}{\partial t} + \rho v C\frac{\partial T}{\partial x} = \frac{1}{\mu^2\sigma}\left[\left(\frac{\partial B}{\partial x}\right)^2 + \left(\frac{\partial B}{\partial y}\right)^2\right] + \frac{\partial\kappa}{\partial T}\left(\frac{\partial T}{\partial x}\right)^2 + \frac{\partial\kappa}{\partial T}\left(\frac{\partial T}{\partial y}\right)^2 + \kappa\frac{\partial^2 T}{\partial x^2} + \kappa\frac{\partial^2 T}{\partial y^2}. \tag{5}$$

Equation (5) can be obtained from standard energy-conservation principles. The meaning of the various terms which appear in the equation are rather obvious except perhaps for the term enclosed in brackets on the right-hand side. If, however, we use equation (3), we can identify this term as being equal to $J^2/\sigma$; consequently, it accounts for resistive heating in the armature and rails.

4

Equations (4) and (5) are the basic differential equations which must be solved subject to some set of initial and boundary conditions. It is evident upon examination of the equations that, provided the initial conditions satisfy the conditions $B(y) = B(-y)$ and $T(y) = T(-y)$, symmetry about $y = 0$ will persist for all time. We will restrict ourselves to this case and only solve the equations for $y \geq 0$. We will assume that there is no transfer of heat from the railgun or armature to the atmosphere surrounding them. Consequently, we take for the boundary conditions on $T$ at each conductor surface the relation

$$\hat{n} \cdot \nabla T = 0, \tag{6}$$

where $\hat{n}$ is the unit normal to the surface (pointing into the conductor). Such a condition also applies along the centerline $y = 0$ from symmetry.

Boundary conditions on the magnetic induction can be easily determined by arguments with Ampere's law. If we denote by $j$ the current per unit rail height, we must have in the inner bore to the left of the armature $B = 2\mu j$, and to the right $B = \mu j$. The latter condition also applies along the upper surface of the inner rail, and along the centerline we must have from symmetry $\partial B/\partial y = 0$. At the ends of the rail, we have taken the condition on the induction to be $\partial B/\partial x = 0$. This condition implies that the current is parallel to the rail surface at these points and is strictly accurate only if the ends are sufficiently far from the armature. The validity of the assumption, as well as an alternate approach for handling these boundary conditions, has been discussed in previous work (Powell, Walbert, and Zielinski 1993). Generally, the rails and armature consist of different materials and under such a circumstance $\partial B/\partial y$ and $\partial T/\partial y$ are not continuous across the rail-armature interface. The appropriate jump conditions were derived previously (Powell, Walbert, and Zielinski 1993) and can be written

$$\left[ \frac{1}{\sigma} \frac{\partial B}{\partial y} \right]_{interface} = 0, \tag{7}$$

where the brackets (here only) denote the change in the enclosed quantity as the interface is crossed. A similar relation for the temperature holds if $B$ is replaced by $T$ and $1/\sigma$ by $\kappa$.

We finally consider the calculation of the induction field in regions of the armature which are bounded on all sides by conducting surfaces. Such a region is indicated, for example, between the front and back contacts of the armature in Figure 1. Since the conductivity in this region is zero, it follows from equations (1)–(3) that $B$ here is independent of position. We denote the constant value by $B_H$, the area of the region by $A_H$, and integrate equation (2) over the area. Application of Stokes' theorem then yields the relation

$$A_H \frac{dB}{dt} = -\int_C \frac{\vec{J}}{\sigma} \cdot d\vec{\ell}, \tag{8}$$

where the integration denotes a line integral in the counterclockwise direction around the periphery of the defining area. In obtaining this result, we have used equation (3) as well as the fact that the tangential component of $\vec{E}$ must be continuous along the line of integration. The constraint imposed by equation (8) is sufficient to determine the time evolution of the spatially constant induction $B_H$.

Equations (4), (5), and (8) with the indicated boundary conditions are sufficient for determining all electrodynamic properties as well as the temperature as a function of both space and time within the rails and the armature. We have previously developed an implicit, finite-difference code for solving the relevant partial differential equations. This code has now been extended to treat augmented railguns and reasonably complicated armature geometry. The details of the numerics have been discussed elsewhere (Powell, Walbert, and Zielinski 1993) and are not repeated here.

## 3.  CALCULATIONS

We now discuss two calculations that we have done to analyze current and heat transport in the armature developed by the University of Texas Center for Electromechanics (UT-CEM) in the CCEMG Program. The planar cross section of the armature appears as shown schematically in Figure 1. This armature is designed to reach a launch velocity of 1.85 km/s via application of a half cycle of a sinusoidal current pulse applied to a series-augmented railgun. The pulse has a duration of 2 ms with a peak current of 780 kA. In the first case undertaken here, the armature is accelerated to 1.85 km/s; in the second, the armature is held fixed so that we can examine directly the effects of velocity upon the resulting magnetic induction and temperature profiles.

As is well known, two-dimensional models directly applied severely overestimate the Lorentz forces and, consequently, the acceleration imparted to the projectile even in simple railguns. The effect is considerably exacerbated in augmented guns. There have been developed some rather *ad hoc* approximations (Batteh 1984) for reducing the magnitude of these forces, and these approximations work reasonably well for simple railguns in the steady state. They cannot, however, be expected to work in the transient case. In an effort not to overestimate both the Lorentz force and the Ohmic heating at early times, we have scaled the current per unit rail height down appropriately to obtain the correct acceleration for a truly two-dimensional, infinite rail-height launcher. More specifically, we assumed a current

6

profile identical in form to that in the actual design, namely,

$$j = j_0 sin(\pi t/t_0), \tag{9}$$

and then calculated the amplitude $j_0$ so that the two-dimensional armature reached a final velocity of 1.85 km/s in a time $t_0$ of 2 ms. The value obtained for $j_0$ was 16.1 MA/m.

Numerical calculations were then carried out for an aluminum armature and copper rails. Temperature-dependent material properties for these metals have been given in our earlier report (Powell, Walbert, and Zielinski 1993). We now discuss some of the more significant results of the calculations.

Shown in Figure 2 are lines of constant magnetic induction at 1 ms (peak current) and at the termination of the pulse at 2 ms. Only the top half of the armature is shown, since there is symmetry about the y axis. The corresponding armature velocities at these times were 925 and 1,850 m/s. It is possible to prove from Maxwell's equations that current cannot cross lines of constant induction so these lines also represent streamlines of the current profile. At 1 ms, when the total current is maximum, a phenomenon known as the velocity skin effect is very apparent from the curvature of the field lines toward the left at the rail-armature interface. In the back contact, the current is directed in the positive y direction and very much concentrated toward the back of the contact. This concentration of current arises at even moderate velocities (Long 1986) because there is insufficient time for current to diffuse into the rails during the time the armature is in contact with a given point on the rail surface. For example, we can crudely estimate from the well-known skin-depth formula, $\delta = (\pi t/\mu\sigma)^{1/2}$, that for a stationary armature current will diffuse into the rails a distance of approximately 1 cm during the 2-ms time of the current pulse. Consequently, the mean "diffusion velocity" is only about 5 m/s, and at armature velocities of only a few tens of meters per second, new rail is being encountered too fast for the current to diffuse enough to produce any appreciable skin depth. Consequently, the resistance along the interface remains high, and the current remains confined to the corner. In the front contact, the current is in the opposite direction, and here the velocity tends to *enhance* the transport of current across the contact at points near the interface. At points far from the interface, however, the current is still largely confined to the front and back sides of the armature at this fairly early time. At 2 ms, when the total current has vanished, considerably more diffusion into the armature has occurred. It should be noted that there is significant magnetic energy in the armature because of eddy currents even at the termination of the pulse. This energy results primarily from the fairly rapid rise time and decay of the sine wave. It should also be observed that the hollow region in the armature between the contacts is effective in enhancing the rate of
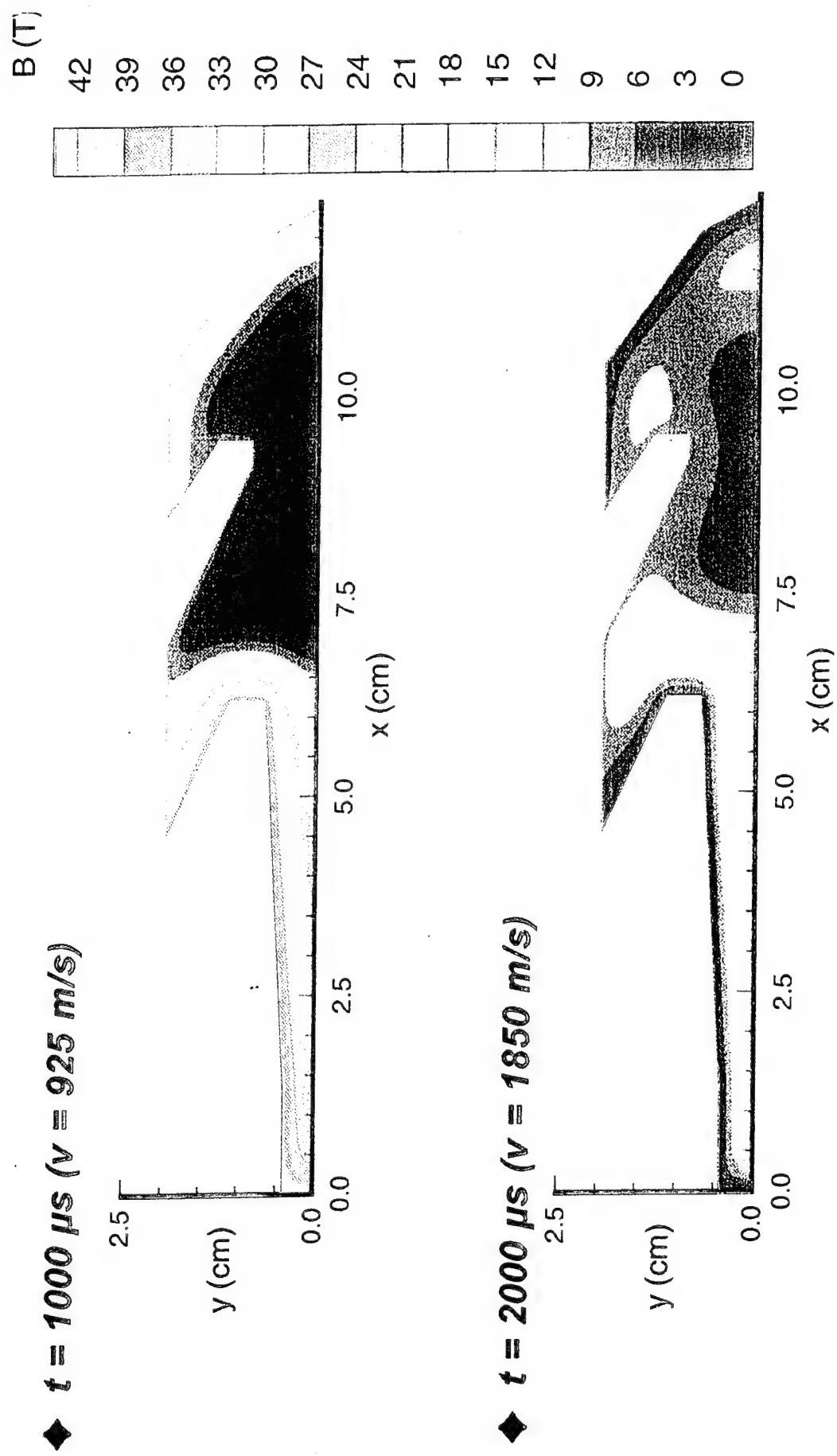
7

Figure 2. Lines of Constant Magnetic Induction in the Armature.

8

diffusion across the armature since this region has negligible conductivity. The induction field in this region is not shown in the figure.

Shown in Figure 3 are isotherms at 2 ms, the termination of the current pulse, when the final armature velocity was 1,850 m/s. Shown for comparison are results of an identical calculation except that the armature was arbitrarily held at rest ($v = 0$). No phase change was taken into account in the model even though at some few points the melting temperature of aluminum ($\simeq 930$ K) was exceeded. Here again the velocity skin effect is quite evident from the substantially greater heating that occurs at the left-hand edge of the rail-armature interface (i.e., the rear contact) for the calculation in which the velocity was accounted for. Clearly, there is significantly greater heating on the left side of the armature than on the right because of the much larger eddy current, particularly at early times. Toward the interior of the armature, the current is sufficiently small and of sufficiently short duration that negligible heating occurs. It should also be observed that there is enhanced heating at sharp corners in the armature where the angle measured in the conductor is greater that 180 degrees. This effect has been noted in our previous work (Powell, Walbert, and Zielinski 1993).

Further demonstration of the importance of the velocity skin effect can be seen in Figure 4 in which the force loading in the armature is plotted at peak current (t=1 ms) for both $v = 0$ and $v=925$ m/s. The force density indicated is simply the magnitude of $\vec{J} \times \vec{B}$. At local points this force has both $x$ and $y$ components but, when averaged over the armature, produces a net result which has only an $x$ component and accelerates the projectile down the barrel of the gun. As is evident in the figure, the large current concentration at the left-most corner of the rail-armature interface when $v \neq 0$ produces significantly greater forces in that region than occur in the $v = 0$ case. Similarly, the forces in the right contact near the interface are larger when $v \neq 0$ because of the transport of current across the contact near the interface. At points far removed from the interface, the force distribution looks much the same in the two cases as does the temperature distribution for the two cases discussed in Figure 3.

To illustrate more qualitatively some of the previously mentioned observations we have plotted in Figure 5 the total magnetic energy per unit rail height, $E_m$, in the armature and, in Figure 6, the current per unit rail height in the front and back contacts. The quantities are given as functions of time throughout the course of the current pulse. For both plots we present results which account for the velocity of the armature as well as results for the calculation in which the armature was held at rest. The magnetic energy per unit rail height was calculated from the expression

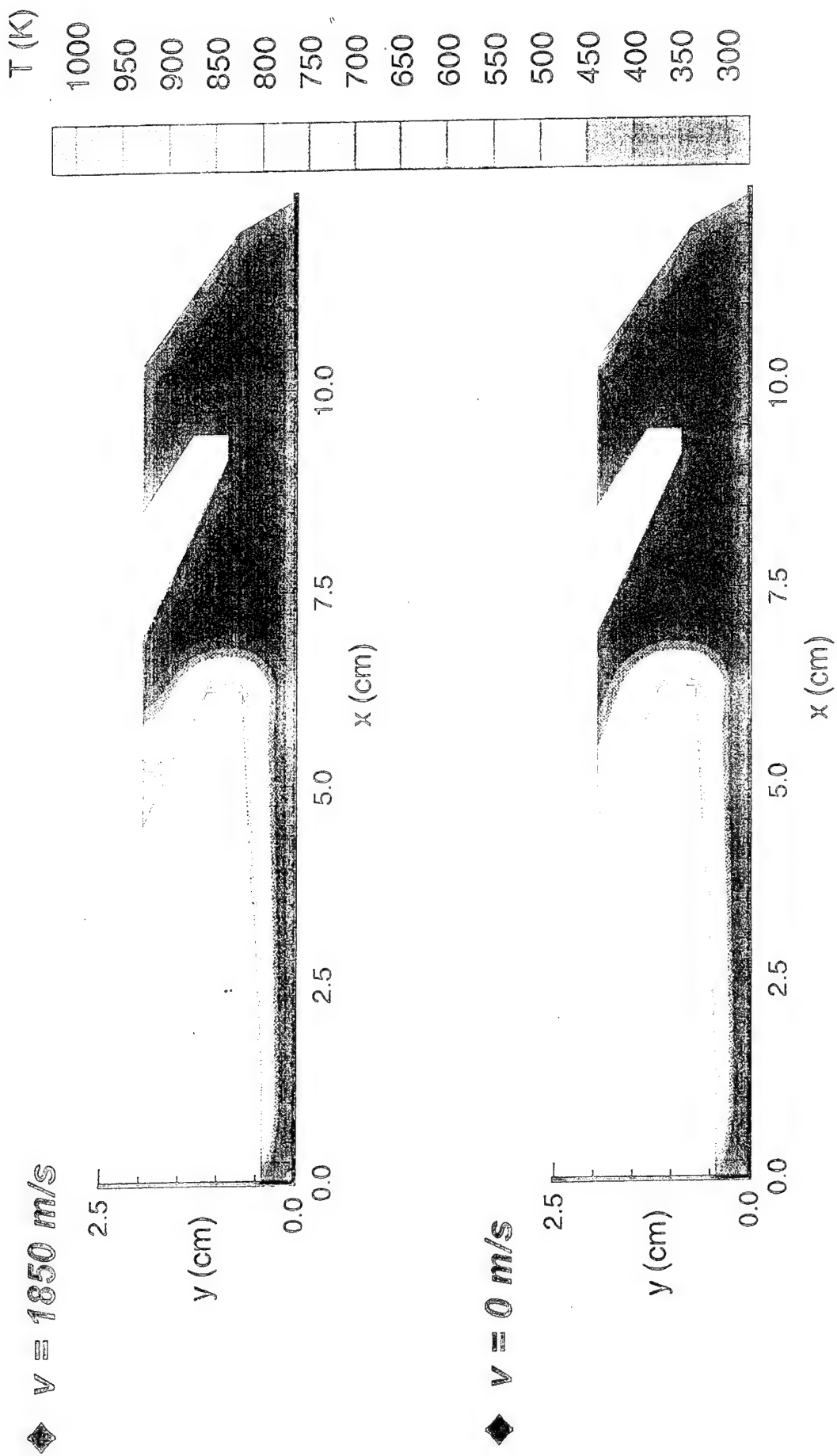$$E_m = \int \frac{B^2}{2\mu} dx\, dy, \tag{10}$$

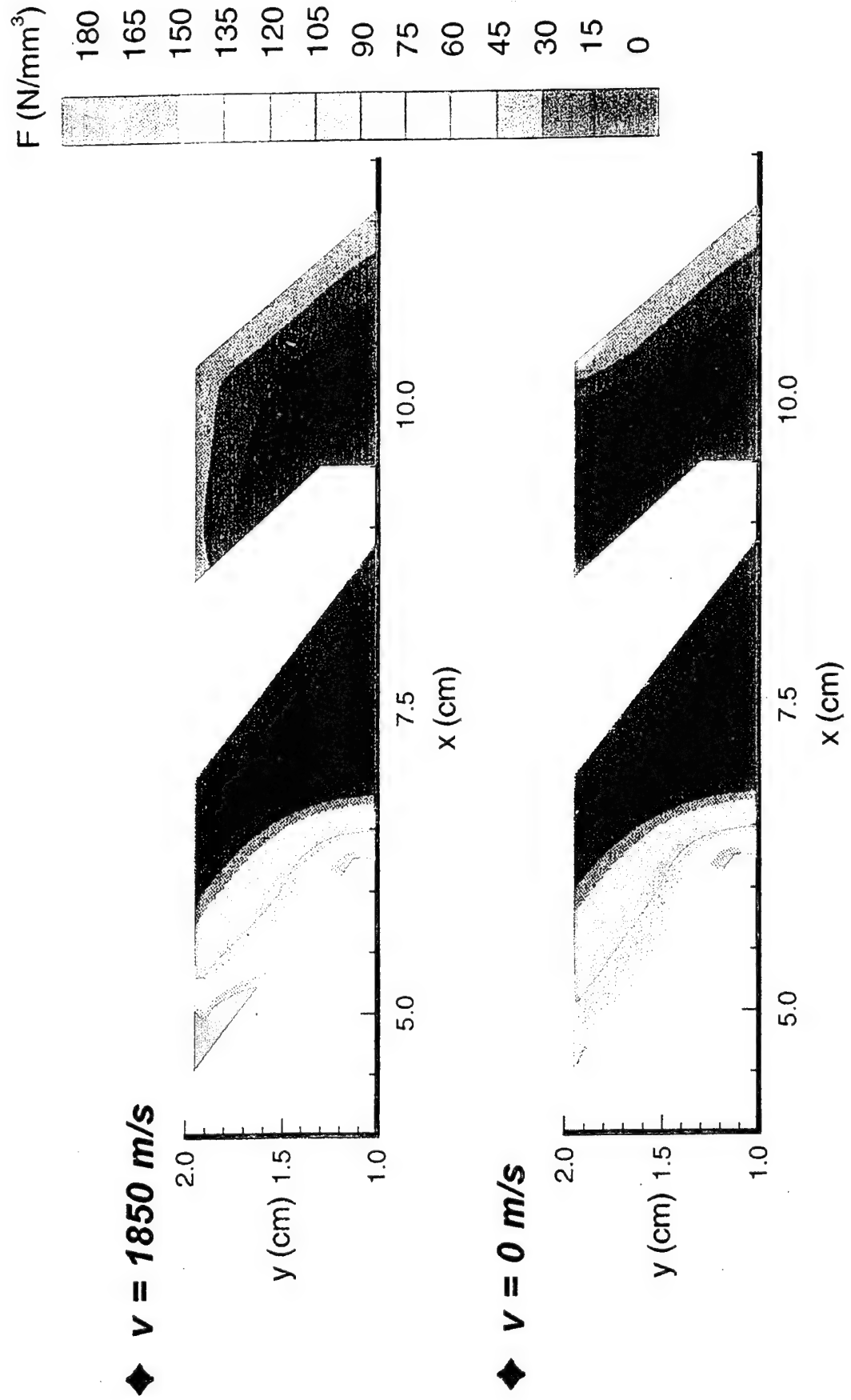9

Figure 3. Isotherms in the Armature at 2 ms.

Figure 4. Force Density in the Armature at 1 ms.

with the integration being taken over the planar cross-sectional area of the armature. The current per unit rail height through the contacts (directed in the $y$ direction) can be obtained by integrating equation (1) from the trailing to the leading edge on the contact in question. If we normalize the resulting values by the total current per unit rail height $j$, we have

$$j_F' = j_F/j = B_H/\mu - 1$$
$$j_R' = j_R/j = 2 - B_H/\mu, \tag{11}$$

where F and R denote the front and rear contacts, respectively.

As is evident in Figure 5, the peak magnetic energy lags the peak current (not shown), which occurs at 1 ms by several hundred microseconds. Furthermore, there is a significant amount of magnetic energy ($\simeq 45$ kJ/m) stored in the armature after the current pulse has ceased. This energy arises from eddy currents which in turn are caused by the inability of the armature to respond to the current in a quasi-stationary manner. At early times when the velocity is small, both curves in Figure 5 yield essentially the same results. At later times the magnetic energy is slightly higher when $v \neq 0$ compared to the no-velocity case. Presumably, the higher value results from the enhanced transport of the augmentation field across the interface from right to left when $v \neq 0$. We have actually carried the calculation out an additional 250 $\mu$s with $j = 0$, i.e., to 2,250 $\mu$s, for the no-velocity case and found that the energy had decayed to about 15 kJ/m at that time. This value represents about 5% of the peak value. Although the amount of magnetic energy stored in the armature at the termination of the current pulse is relatively small, the resultant deflections and stresses may perturb the armature and affect the discard of the sabot. This phenomenon is beyond the scope of this study and requires further investigation.

In Figure 6 are shown the normalized current per unit rail height in the the front and back contacts, $j_F'$ and $j_R'$, as a function of time. The negative signs are indicative of current directed in the negative y direction and, of course, $j_F' + j_B' = 1$. At early times, the magnitude of the current through the back contact is exactly twice that through the front. This behavior results from the larger induction field at the back and the negligible amount of current transport across the armature. It is particularly noteworthy that for the case of no velocity the current distribution is fairly constant during the time of the current pulse. However, when the velocity is accounted for, the transport of current from the front toward the back surface leads to a much more uniform distribution. In fact, at the very latest times there is nearly an equal amount of current through the front and back contacts, and both are positively directed. Irrespective of direction, the current partition at the back and front contacts is roughly 2:1 for the $v = 0$ case. For the case with velocity, the back and front
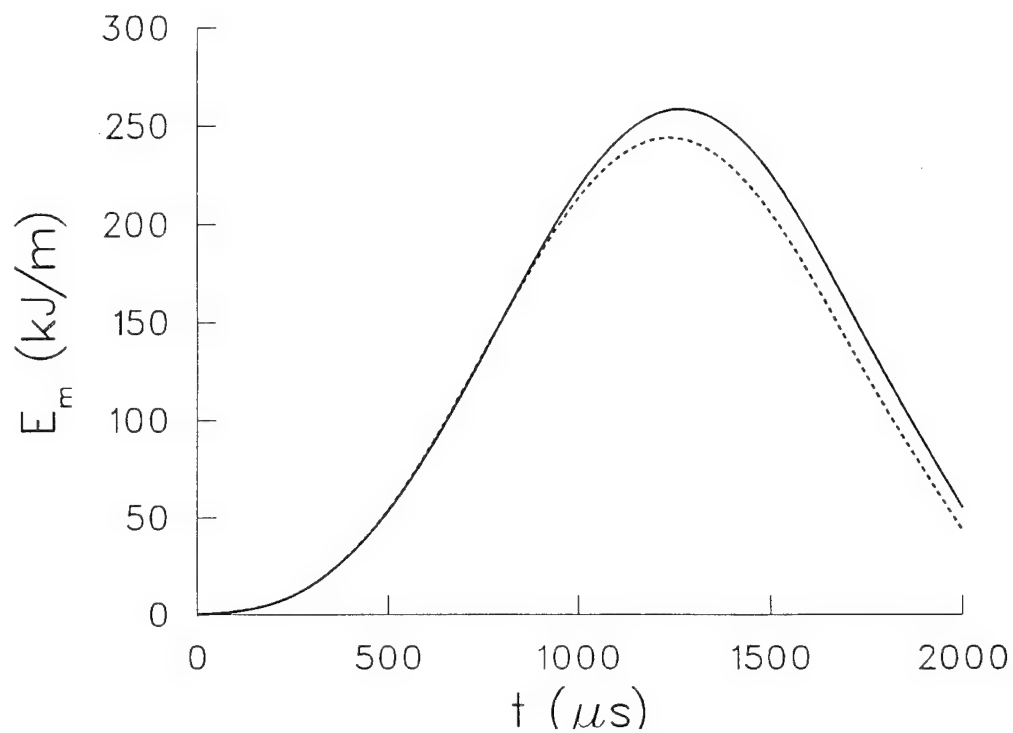
12

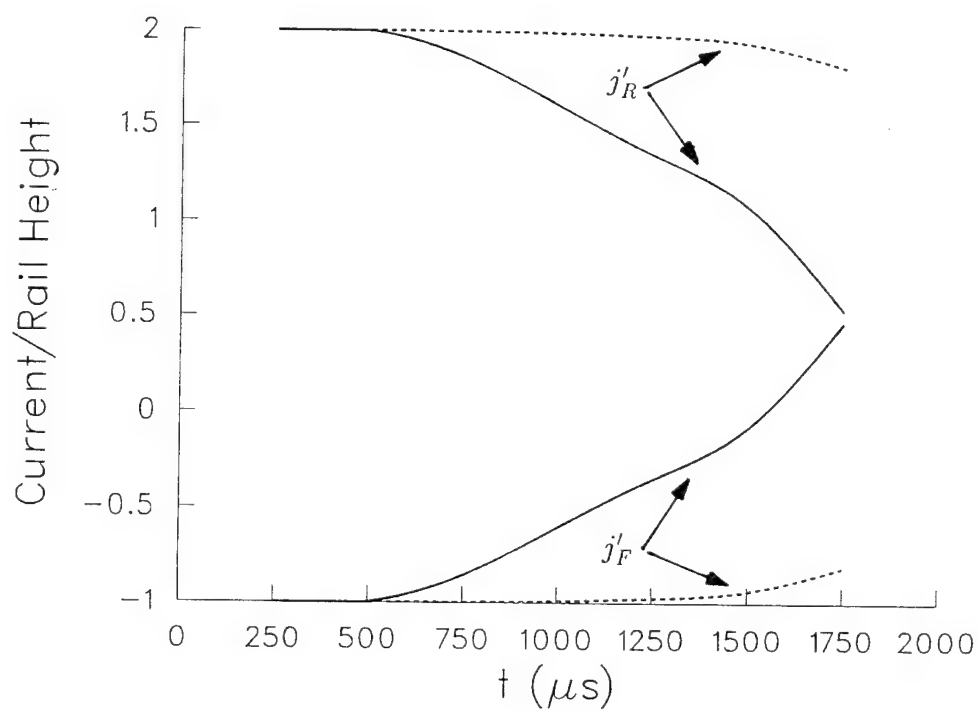**Figure 5.** Magnetic Energy in the Armature. (Solid, $v \neq 0$; Dotted, $v = 0$).



**Figure 6.** Normalized Current per Unit Rail Height in Contacts. (Solid, $v \neq 0$; Dotted, $v = 0$).

13

contact current partition is more time-dependent and reaches a maximum of 4:1 shortly after peak current.

In Figure 7 are shown a series of isotherms in the rail at 500-$\mu$s intervals. For presentation, we have transformed these results to the reference frame in which the rails are fixed. That transformation is accomplished via the relation $X = x - x_{end}$, where $x_{end}$ denotes the location of the left-most end of the rail at the time in question. The armature, not shown in this figure, is located very near the right-most end of the rail (see Figure 8); the part of the rail farther to the right is excluded from the figure. There is some heating at the top of the rail resulting from the diffusion of the augmenting field ($B = \mu j$ at the upper surface) downward. More significant, however, is the heating of the inner-bore surface of the rail. The larger temperatures there result both from the larger induction field at the surface (B=2 $\mu j$), as well as the large current concentration at the interface corner of the armature contact. Clearly, the amount of heating depends upon the past history of the current profile, as well as the speed of the armature as it passed the point in question. In particular, high induction fields produce high currents and significant Ohmic heating; high velocities produce large relative current concentration at the interface corner, but small dwell times in the vicinity of a given point in space. Thus, at late times, when the velocity is high and the current is decreasing rapidly, relatively little heating near the rail-armature interface occurs. It should also be noted that there is insignificant heating in the interior of the rail. This result suggests that there is incomplete penetration of the current across the rail thickness, a distance of 2 cm.

We finally show in Figure 8 an enlarged view of the rail isotherm at peak current. Only the first 5 mm above the bore surface of the rail is shown. (It should be noted that the armature is not drawn to scale in the $y$ direction.) More detail is evident than exists in the previous figure, and the profiles closely resemble those discussed in our previous work (Powell, Walbert, and Zielinski 1993). It is noteworthy that the maximum temperature at the rail surface is only about 700 K, and thus lower than both the melt temperature of copper and the temperature at "hot spots" in the armature. While this temperature rise is of minor concern for the single-shot computations discussed here, CCEMG is a multishot system, and the resulting long-term temperature effects need further study.

## 4. SUMMARY AND CONCLUSIONS

We have employed a two-dimensional model to investigate current and heat transport in an armature developed by UT-CEM in the CCEMG Program. The armature is accelerated to 1.85 km/s in a series-augmented railgun. Time-dependent calculations were carried out
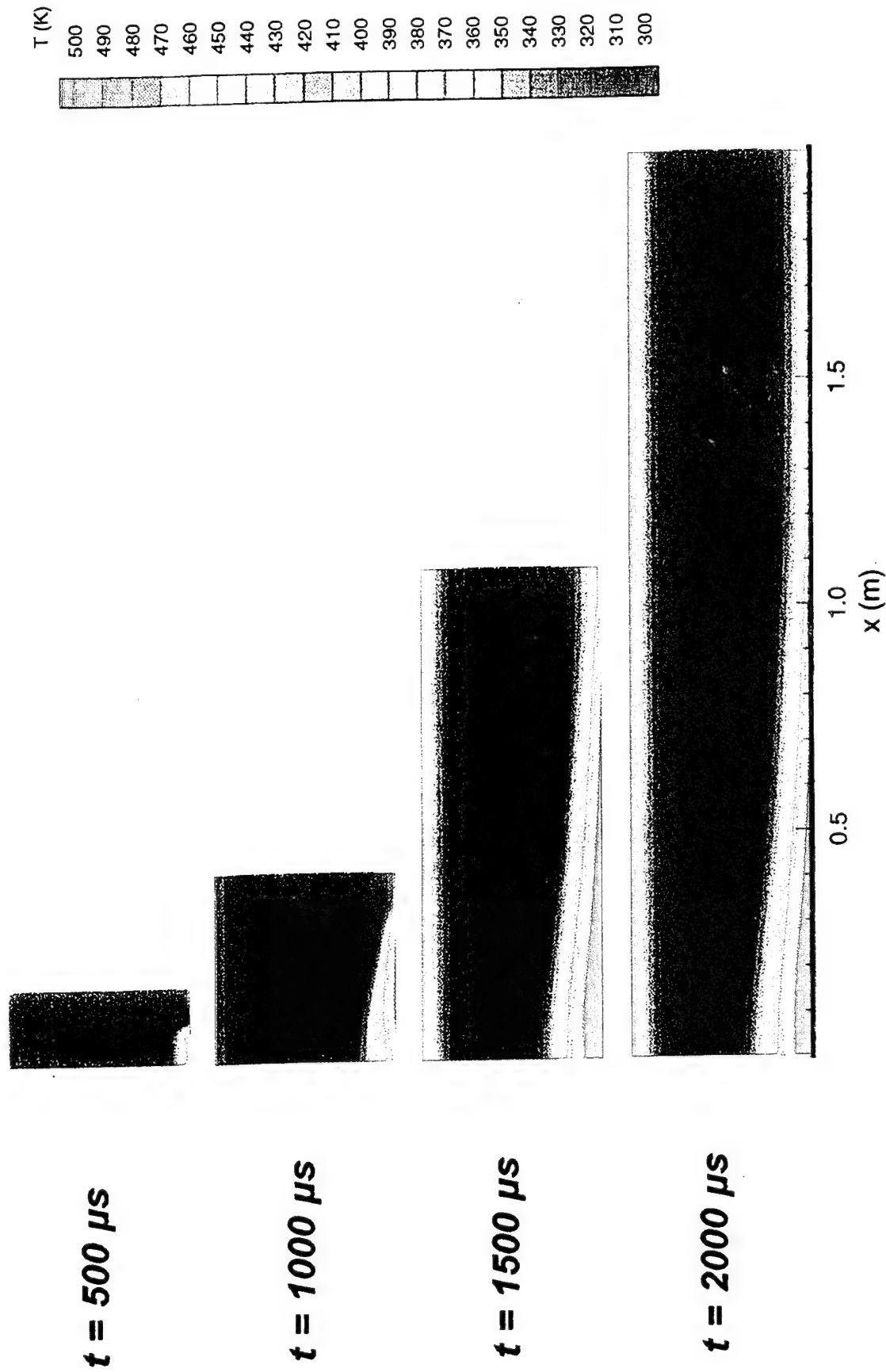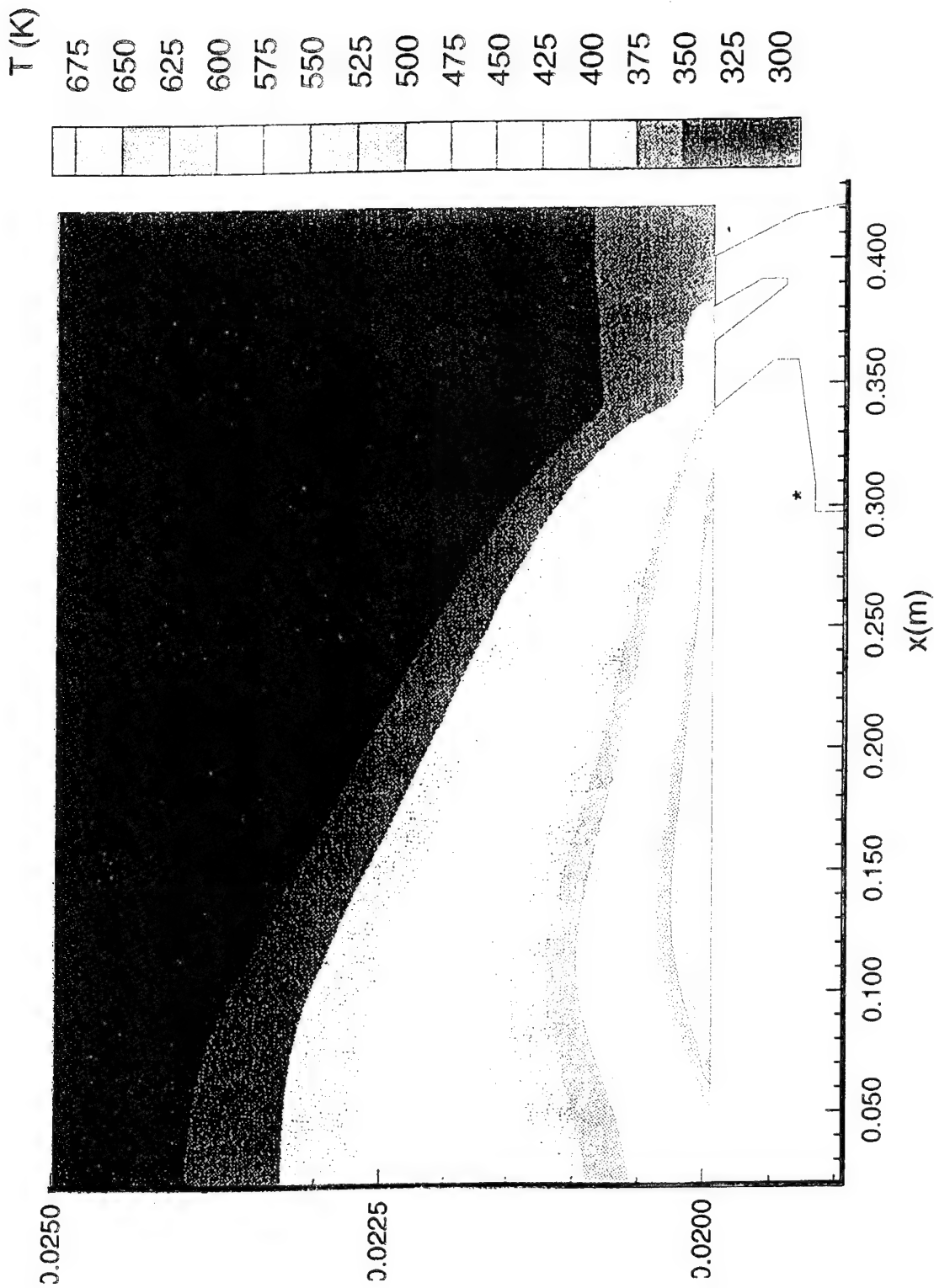
Figure 7. Isotherms in the Upper Rail as a Function of Time.

Figure 8. Enlarged View of Isotherms in Upper Rail at 1 ms.

\* **Note: Armature not drawn to scale in the y direction.**

for the duration of the current pulse with the armature motion accounted for and compared with calculations in which the armature was held fixed. General conclusions reached as a result of this analysis can be reiterated as follows.

(1) The velocity skin effect is significant at points near the rail-armature interface at even moderate velocities. At points far removed from the interface, the effect is small and the induction and temperature profiles appear similar to those for the no-velocity calculation.

(2) There is significant thermal and force loading at the left-hand corner of the rail-armature interface because of the high current density produced by the velocity skin effect. In addition, there is significant heating and force loading at large-angle corners within the armature.

(3) Near the rail-armature interface, the transport of the augmenting induction field across the armature is enhanced by both the velocity skin effect and by the hollow region between the contacts. For the case of no velocity, however, or at points far removed from the interface, there is insufficient time during the shot for the field to diffuse completely across the armature.

(4) The fast rise time and decay of the current pulse lead to some magnetic energy remaining in the armature (and rails) at the termination of the pulse.

(5) Thermal loading in the rails is small relative to that at localized points in the armature. However, a region of the rail surface near the breech reaches temperatures of about 700 K for the single shot considered.

There are obviously significant limitations with the use of two-dimensional models for quantitative predictions in real railguns with finite rail height. We do believe, however, that these calculations are useful for obtaining a qualitative understanding of how these devices operate and for studying physical phenomena associated with them. Primary among these phenomena is the physics which occurs at the rail-armature interface. Because of the high relative velocities at that boundary as well as the existence of a sharp corner on the left-hand side of the armature, we have been unable to accurately resolve the temperature and field profiles near that corner. The problem exists in a region of only a few grid points near the corner and is probably not too important for the problem studied here. However, in future calculations in which phase changes are accounted for, melting is likely to always occur near such a sharp corner, and it is important to obtain accurate predictions near that point. It seems likely that alternate numerical techniques as well as superior models for handling the interface physics are likely to be required. We are investigating these techniques at the present time.

## 5. REFERENCES

Batteh, J. H. "Momentum Equation for Arc-Driven Rail Guns." *Journal of Applied Physics*, vol. 56, p. 3182, 1984.

Hsieh, K. T. "A Lagrangian Formulation for Mechanically, Thermally Coupled Electromagnetic Diffusive Processes with Moving Conductors." Paper presented at the Seventh Electromagnetic Launch Symposium, San Diego, CA, April 1994.

Hughes, W. F., and F. Y. Young. "Transient and Steady-State Performance of the Laminated Armature for the Electromagnetic Armature." Air Force Armament Laboratory EM Gun Armature Workshop, Eglin AFB, FL, June 1986.

Kitzmiller, J. R., S. B. Pratap, T. A. Aanstoos, K. G. Cook, R. A. Kuenast, B. T. Murphy, and D. R. Perkins. "Optimization and Critical Design Issues of the Air Core Compulsator for the Cannon Caliber Electromagnetic Launcher System (CCEML)." Paper presented at the Seventh Electromagnetic Launch Symposium, San Diego, CA, April 1994.

Long, G. C. "Railgun Current Density Distributions." *IEEE Transactions on Magnetics*, vol. MAG-22, p. 1597, 1986.

Long, G. C. "Fundamental Limits to the Velocity of Solid Armatures in Railguns." Doctoral Dissertation, University of Texas at Austin, Publication Number TD-35, 1987.

Nearing, J. C., and M. A. Huerta. "Skin and Heating Effects of Railgun Current." *IEEE Transactions on Magnetics*, vol. MAG-25, p. 381, 1989.

Powell, J. D, D. J. Walbert, and A. E. Zielinski. "Two-Dimensional Model for Current and Heat Transport in Solid-Armature Railguns." ARL-TR-74, U. S. Army Research Laboratory, Aberdeen Proving Ground, MD, February 1993.

Putley, D. "Preliminary Investigations of the Velocity Skin Effect Using the PE2D Code." Presented at the Seventh ELA Meeting, Milpitas, CA, December 1989.

Rodger, D. and P. J. Leonard. "Alternative Schemes for Electromagnetic Modeling of Rail Guns at Speed Using Finite Elements." *Proceedings of the Third European Symposium on EML Technology*, London, England, 1991.

Rodger, D., P. J. Leonard, and J. F. Eastman. "Modeling Electromagnetic Rail Launchers at Speed Using 3D Finite Elements." *IEEE Transactions on Magnetics*, vol. MAG-27, p. 314, 1991.

Rodger, D., P. J. Leonard, J. F. Eastman, and S. P. Atkinson. "3D Finite Element Modeling of Electromagnetic Launchers." *Proceedings of the Second European Symposium on EML Technology*, ISL St. Louis, France, 1989.

Young, F. Y. and W. F. Hughes. "Rail and Armature Current Distributions in Electromagnetic Launchers." *IEEE Transactions on Magnetics*, vol. MAG-18, p. 33, 1982.

Yun, H. D. and J. H. Price. "Electromagnetic and Structural Analyses of Electric Gun and Integrated Launch Package Systems." Paper presented at the Seventh Electromagnetic Launch Symposium, San Diego, CA, April 1994.

NO. OF
COPIES    ORGANIZATION

2    ADMINISTRATOR
ATTN DTIC DDA
DEFENSE TECHNICAL INFO CTR
CAMERON STATION
ALEXANDRIA VA 22304-6145

1    DIRECTOR
ATTN AMSRL OP SD TA
US ARMY RESEARCH LAB
2800 POWDER MILL RD
ADELPHI MD 20783-1145

3    DIRECTOR
ATTN AMSRL OP SD TL
US ARMY RESEARCH LAB
2800 POWDER MILL RD
ADELPHI MD 20783-1145

1    DIRECTOR
ATTN AMSRL OP SD TP
US ARMY RESEARCH LAB
2800 POWDER MILL RD
ADELPHI MD 20783-1145


ABERDEEN PROVING GROUND

5    DIR USARL
ATTN AMSRL OP AP L (305)

| NO. OF<br>COPIES | ORGANIZATION |
|---|---|
| 2 | COMMANDER<br>ATTN SMCAR FSA E<br>DR T GORA<br>J BENNETT<br>US ARMY ARDEC<br>PCNTY ARSNL NJ 07806-5000 |
| 4 | COMMANDER<br>ATTN SMCAR CCL FA<br>H MOORE<br>LTC GERASIMAS<br>W WILLIAMS<br>B SCHLENNER<br>US ARMY ARDEC<br>BLDG 65N<br>PCNTY ARSNL NJ 07806-5000 |
| 2 | DIRECTOR<br>ATTN SMCAR CCB RT MICK CIPOLLO<br>SMCAR CCM RM DR PAT VOTTIS<br>BENET LABORATORIES<br>WATERVLIET NY 12189 |
| 3 | CG MCRDAC<br>ATTN CODE AWT<br>C VAUGHN<br>G SOLHAND<br>MAJ F WYSOCKI<br>QUANTICO VA 22134-5080 |
| 1 | WL MNSH<br>ATTN DONALD M LITTRELL<br>SITE A15<br>EGLIN AFB FL 32542-5434 |
| 1 | DIRECTOR<br>ATTN R S HAWKE L 153<br>LAWRENCE LIVERMORE NATL LAB<br>PO BOX 808<br>LIVERMORE CA 94550 |
| 1 | GA TECHNOLOGIES INC<br>ATTN L HOLLAND<br>PO BOX 85608<br>SAN DIEGO CA 92138 |
| 1 | ELECTROMAGNETIC RESEARCH INC<br>ATTN PETER MONGEAU<br>2 FOX ROAD<br>HUDSON MA 01749 |

| NO. OF<br>COPIES | ORGANIZATION |
|---|---|
| 2 | IAP RESEARCH INC<br>ATTN JOHN P BARBER<br>DAVID P BAUER<br>2763 CULVER AVE<br>DAYTON OH 45429-3723 |
| 2 | SCIENCE APPLICATIONS INTL CORP<br>ATTN K A JAMISON<br>G ROLADER<br>1247 B NORTH EGLIN PARKWAY<br>SHALIMAR FL 32579 |
| 1 | UDLP<br>ATTN BRAD GOODELL<br>MAILSTOP M170<br>4800 E RIVER ROAD<br>MINNEAPOLIS MN 55421-1498 |
| 2 | SCIENCE APPLICATIONS INTL CORP<br>ATTN JAD H BATTEH<br>L THORNHILL<br>1503 JOHNSON FERRY RD SUITE 100<br>MARIETTA GA 30062 |
| 1 | WESTINGHOUSE SCIENCE & TECHLGY CTR<br>ATTN DOUG FIKSE<br>1310 BEULAH ROAD<br>PITTSBURGH PA 15233 |
| 1 | AUBURN UNIVERSITY<br>ATTN EUGENE CLOTHIAUX<br>206 ALLISON LAB<br>AUBURN UNIVERSITY AL 36849-5311 |
| 1 | TEXAS TECHNICAL UNIVERSITY<br>ATTN M KRISTIANSEN<br>DEPT OF EE COMPUTER SCIENCE<br>LUBBOCK TX 79409-4439 |
| 5 | INSTITUTE FOR ADVANCED TECHLGY<br>ATTN H FAIR<br>KT HSIEH<br>D MCNAB<br>P H SULLIVAN<br>J V PARKER<br>4030 2 W BRAKER LANE<br>AUSTIN TX 78759-5329 |

| NO. OF COPIES | ORGANIZATION |
|---|---|
| 1 | UNIVERSITY OF MIAMI<br>ATTN MANUEL A HUERTA<br>DEPT OF PHYSICS<br>PO BOX 248046<br>CORAL GABLES FL 33124 |
| 1 | NORTH CAROLINA STATE UNIV<br>ATTN JOHN GILLIGAN<br>DEPT OF NUCLEAR ENGRG<br>PO BOX 7909<br>RALEIGH NC 27695 |
| 1 | CTR FOR LASER APP ENGR SCI & MECH<br>ATTN DENNIS KEEFER<br>UNIV OF TENNESSEE<br>SPACE INSTITUTE MAIL STOP 14<br>B H GOETHERT PARKWAY<br>TULLAHOMA TN 37388-8897 |
| 3 | CTR FOR ELECTROMECHANICS<br>ATTN SIDDHARTH B PRATAP<br>JOHN H PRICE<br>HEEDO YUN<br>UNIV OF TEXAS AT AUSTIN<br>10100 BURNET ROAD BLDG 133<br>AUSTIN TX 78748 |
| 1 | LORAL VOUGHT SYSTEMS<br>ATTN ROBERT TAYLOR<br>PO BOX 650003 WT 17<br>DALLAS TX 75265-0003 |

| NO. OF COPIES | ORGANIZATION |
|---|---|
| | ABERDEEN PROVING GROUND |
| 1 | CDR USATECOM<br>ATTN    AMSTE SI F |
| 31 | DIR, USARL<br>ATTN:  AMSRL-W<br>        DR. C. H. MURPHY<br>     AMSRL-WT-WD<br>        DR A. NIILER<br>        DR P. BERNING<br>        DR R. BOSSOLI<br>        DR S. CORNELISON<br>        DR A. GAUSS<br>        DR C. HOLLANDSWORTH<br>        DR C. HUMMER<br>        MR L. KECSKES<br>        DR T. KOTTKE<br>        DR M. MCNEIR<br>        DR J. POWELL (5 CPS)<br>        DR A. PRAKASH<br>        MR C. STUMPFEL<br>        DR G. THOMPSON<br>     AMSRL-WT-WE, DR J. TEMPERLEY<br>     AMSRL-WT-P, MR. A. HORST<br>     AMSRL-WT-PA<br>        MS. G. WREN<br>        MR. G. KATULKA<br>     AMSRL-WT-PB<br>        DR. E. SCHMIDT<br>        MR. A. ZIELINSKI (5 CPS)<br>     AMSRL-WT-PD<br>        DR. W. DRYSDALE<br>        MR. DO HOPKINS |

INTENTIONALLY LEFT BLANK.

# USER EVALUATION SHEET/CHANGE OF ADDRESS

This Laboratory undertakes a continuing effort to improve the quality of the reports it publishes. Your comments/answers to the items/questions below will aid us in our efforts.

1. ARL Report Number ___ARL-MR-258___ Date of Report ___August 1995___

2. Date Report Received _____

3. Does this report satisfy a need? (Comment on purpose, related project, or other area of interest for which the report will be used.) _____

_____

_____

4. Specifically, how is the report being used? (Information source, design data, procedure, source of ideas, etc.)

_____

_____

_____

5. Has the information in this report led to any quantitative savings as far as man-hours or dollars saved, operating costs avoided, or efficiencies achieved, etc? If so, please elaborate. _____

_____

_____

6. General Comments. What do you think should be changed to improve future reports? (Indicate changes to organization, technical content, format, etc.) _____

_____

_____

_____

CURRENT
ADDRESS

Organization _____

Name _____

Street or P.O. Box No. _____

City, State, Zip Code

7. If indicating a Change of Address or Address Correction, please provide the Current or Correct address above and the Old or Incorrect address below.

OLD
ADDRESS

Organization _____

Name _____

Street or P.O. Box No. _____

City, State, Zip Code

(Remove this sheet, fold as indicated, tape closed, and mail.)
**(DO NOT STAPLE)**